Interpreting Photoactivated Fluorescence Microscopy Measurements of Steady-State Actin Dynamics

Y. Tardy,* J. L. McGrath,* J. H. Hartwig,‡ and C. F. Dewey*
*Fluid Mechanics Laboratory, Department of Mechanical Engineering, Massachusetts Institute of Technology, Cambridge, Massachusetts 02139; and ‡ Experimental Medicine Division, Brigham and Women's Hospital and Department of Medicine, Harvard Medical School, Boston, Massachusetts 02115 USA

ABSTRACT A continuum model describing the steady-state actin dynamics of the cytoskeleton of living cells has been developed to aid in the interpretation of photoactivated fluorescence experiments. In a simplified cell geometry, the model assumes uniform concentrations of cytosolic and cytoskeletal actin throughout the cell and no net growth of either pool. The spatiotemporal evolution of the fluorescent actin population is described by a system of two coupled linear partial-differential equations. An analytical solution is found using a Fourier-Laplace transform and important limiting cases relevant to the design of experiments are discussed. The results demonstrate that, despite being a complex function of the parameters, the fluorescence decay in photoactivated fluorescence experiments has a biphasic behavior featuring a short-term decay controlled by monomer diffusion and a long-term decay governed by the monomer exchange rate between the polymerized and unpolymerized actin pools. This biphasic behavior suggests a convenient mechanism for extracting the parameters governing the fluorescence decay from data records. These parameters include the actin monomer diffusion coefficient, filament turnover rate, and ratio of polymerized to unpolymerized actin.

INTRODUCTION

Actin filaments are key structural components of cells. They are organized into cortical networks and bundles that maintain cell shape and fill all cellular protrusions such as lamellapodia, filopodia, and membrane ruffles. They are also highly dynamic. Purified actin at cellular concentrations and physiological salts and temperature spontaneously assembles into filaments. Under these conditions, monomers are thought to flux through filaments from the barbed to pointed direction as a consequence of the different affinities for monomers of the two filament ends. This process has been called treadmilling (Wegner, 1976). This picture implies that filaments are regularly refurbished, or "turned over," with a fresh supply of monomer subunits.

Because of the presence of actin binding proteins it is unclear whether treadmilling occurs in cells; however, filament turnover still occurs. In most eukaryotic cells, irrespective of whether the cells are stationary or moving, only ≈50% of the total cellular actin is assembled into filaments (Bray and Thomas, 1976; Condeelis, 1992). Unpolymerized actin is maintained in a non-polymerizable pool by stoichiometric interactions with soluble proteins such as thymosin β-4 (Nachmias, 1993; Safer et al., 1990), profilin (Lassing and Lindberg, 1985), cofilin, and others (see Sun et al. (1995) for a review). These monomer-sequestering proteins function in combination with proteins that cap the barbed ends of actin filaments to regulate the assembly kinetics of actin (Hartwig, 1992; Carlier et al., 1993). Experiments have shown that filaments in both resting and moving cells are highly dynamic and that actin in the unpolymerized pool is constantly being exchanged into the filamentous pool as cytoplasmic polymers undergo cycles of assembly-disassembly. Such evidence of filament turnover has been obtained from incorporation studies of microinjected fluorescently labeled actin (Kries et al., 1979; Taylor and Wang, 1978), from fluorescence recovery patterns in fluorescence recovery after photobleaching studies (FRAP) (Wang, 1985), and more recently from fluorescence decay data in photoactivated fluorescence (PAF) studies (Theriot and Mitchison, 1991, 1992).

Steps toward a quantitative characterization of actin dynamics in vivo have been made in studies measuring the diffusion of cytosolic actin monomer and the turnover rate of actin filaments. Investigators have attempted to measure these processes individually using PAF and FRAP (Wang et al., 1982; Kreis et al., 1982; Theriot and Mitchison, 1991, 1992). FRAP studies on monomer diffusion have employed the measurement protocol of Axelrod et al. (1976). The theoretical development behind this protocol, however, considers self-diffusion and convection of a fluorescent species in an infinite domain and is inappropriate for measurements on cytoskeleton proteins because filament dynamics have not been considered. In previous PAF turnover measurements the experimental data have been interpreted assuming no contribution from monomer diffusion (Theriot and Mitchison, 1991, 1992). Currently, turnover times are reported as half-times for fluorescence decay in PAF studies (Theriot and Mitchison, 1991). Similarly, the Axelrod et al. (1976) protocol relates half-times for fluorescence recovery to diffusion coefficients. As will be shown in this paper, monomer diffusion and filament turnover both contribute to

Received for publication 9 March 1995 and in final form 31 July 1995.
Address reprint requests to Yanik Tardy at his present address, Biomedical Engineering Laboratory, Swiss Federal Institute of Technology, PSE-Ecublens, 1015 Lausanne, Switzerland. Tel.: 41–21-6938350; Fax: 41–21-6938330; E-mail: tardy@eldp.epfl.ch.

0006-3495/95/11/1674/00 $2.00

the evolution of fluorescence in PAF and FRAP studies and thus half-times for fluorescence decay or recovery may not characterize either of these processes very well.

In the present work, a mathematical model of the actin cytoskeleton in steady-state is presented to guide the interpretation of PAF and FRAP data on cytoskeletal proteins. The model accounts for the interaction of cytosolic actin monomer with filaments and reveals how fluorescence decay records are governed by many parameters including monomer diffusion coefficients, filament turnover rates, and the ratio of polymerized to depolymerization actin.

PAF MICROSCOPY

PAF microscopy has been used recently to estimate filament turnover in living cells (Theriot and Mitchison, 1991, 1992; Mitchison, 1989). In these experiments, actin monomers are labeled with a nonfluorescent fluorophore derivative (caged actin) and microinjected into living cells. After incorporation of the injected actin into the endogenous cytoskeleton, the cell is flashed with a narrow band of UV light, converting the fluorophore in the band back to its fluorescent parent (for a review see Sawin et al., 1992). The subsequent decay of fluorescence in the band is monitored to infer information about protein dynamics.

This technique is the negative analog of FRAP where the resultant image is a dark bleached spot on a bright background (In FRAP the fluorescence of the injected compound is locally quenched with a high power laser beam. The rate of recovery of the bleached spot is used to measure the diffusion coefficient of the fluorescently tagged molecule.). Because the lower light levels used should be less perturbing to the cell and because of an inherent signal-to-noise advantage, we have selected PAF over FRAP as the vehicle to measure the dynamics of actin in our laboratory. The mathematical model presented here is developed from the perspective of a PAF experiment; however, the model may be easily applied to FRAP experiments with fluorescence recovery replacing fluorescence decay.

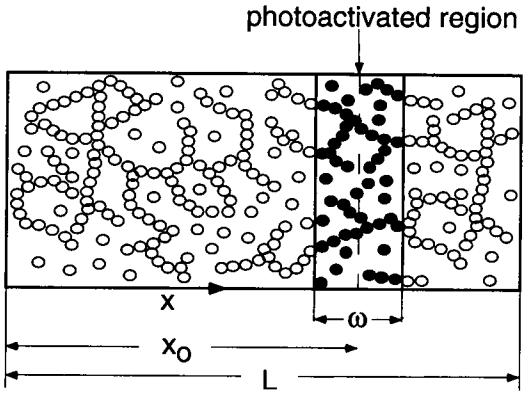

FIGURE 1 Schematic of the model system. The cell cortex is modeled as a rectangular geometry containing two actin pools, free diffusing monomers and nondiffusing filaments. Both monomers and filaments are photoactivated in a narrow band at the beginning of the experiment (●). The fluorescence diffuses out of the band with time. The position of the slit center line is given by x_0 and the slit width is ω.

MATHEMATICAL MODEL

Following are the assumptions of the mathematical model.

1) The cell cortex is modeled as having a rectangular geometry of constant thickness and uniform properties (Fig. 1). The position along the cell is given by the spatial coordinate x. The photoactivated band width is denoted by w and the cell length by L. Given that the photoactivated band will be rectangular and spans the width of the cell, this approach reduces the problem to one dimension. This is the simplest geometric approach that can produce insights concerning the effects of the ends of the cell. Other refinements such as non-uniform thickness or properties (e.g., a nucleus) can be added to the model; these refinements will generally require a numerical solution of the resulting equations.

2) The actin is uniformly distributed across the cell. This ignores the presence of filament bundles as well as gradients in cortical actin (Giuliano and Taylor, 1994). If cortical actin distributions are carefully quantified later, it will be a simple extension of the model to incorporate such data.

3) Two pools of actin are considered, a non-diffusing filamentous pool and a diffusable monomer pool. Filaments are considered immobile. This approach disregards the possibility of short diffusible actin filaments whose diffusion coefficient would be smaller than that of the monomer. However, cortical actin filaments of eukaryotic cells are highly cross-linked; therefore, the number of freely diffusing filaments should be small (Hartwig and Shelvin, 1986). Provided there are no important chemical alterations, e.g., an increase or decrease in actin hydrophobicity, the presence of fluorophore labeling should not affect diffusion coefficients, as the ratio of the molecular weight of actin to that of the caged fluorophore is typically >100. Therefore, all monomers are considered to diffuse alike.

4) There is no net growth of the filamentous or monomeric pool. This is the steady-state assumption, which limits the applicability of the model to situations where there is no net polymerization or depolymerization of the cytoskeleton.

5) Finally, we postulate that the exchange rate of actin subunits between the two pools is uniform throughout the cell. Together with assumption 2, this suggests that filament turnover is uniform throughout the cell. This remains to be shown experimentally, but again we adopt this assumption for simplicity recognizing this as a possible area for future extensions of the model.

Derivation of the dimensional problem

The general equation of species conservation is written for the uncaged (fluorescent) monomer population (the subscript "um") as

$$\frac{D}{Dt}c_{um} = \mathcal{D}\nabla^2 c_{um} + f_{um}. \tag{1}$$

The left side denotes the time rate of change of the concentration of fluorescent monomer in the monomer pool, c_{um}, within a fluid element. The first term of the right side gives the contribution to this rate from monomer diffusion, where $\mathcal{D}$ is the monomer diffusion coefficient. The second term on the right side accounts for the production or loss of fluorescent subunits from the unpolymerized pool (i.e., it accounts for the exchange of actin subunits between the filamentous and monomer pools).

In assumption 2, we assumed no gradient in total monomer concentration (fluorescent + nonfluorescent); therefore, the convective terms in the total derivative are zero. This fact along with the one-dimensional geometry reduces Eq. 1 to

$$\frac{\partial c_{um}}{\partial t} = \mathcal{D}\frac{\partial^2 c_{um}}{\partial x^2} + f_{um}. \tag{2}$$

The filamentous pool is nondiffusing (assumption 3). Since there is no change in the total amounts of monomer or polymer (assumption 4), this pool must undergo a flux of actin subunits of opposite sign to that of the monomer pool. Therefore, the equation governing this population is

$$\frac{\partial c_{uf}}{\partial t} = -f_{um}. \tag{3}$$

Where the concentration c_{uf} is the concentration of fluorescent monomer in the filamentous pool (not the concentration of fluorescent filaments). The probability that a monomer leaving the filamentous pool is fluorescent is given by c_{uf}/c_f. Similarly, the probability that a monomer leaving the monomer pool is fluorescent is given by c_{um}/c_m, where c_m and c_f are the total cellular concentration of monomer in the monomer and filamentous pools respectively. With the uniform rate of monomer exchange between the two pools denoted by $\dot{g}$, this reasoning allows us to cast an expression for f_{um}:

$$f_{um} = \dot{g}\left(\frac{c_{uf}}{c_f} - \frac{c_{um}}{c_m}\right). \tag{4}$$

With this, Eqs. 2 and 3 become, respectively,

$$\frac{\partial c_{um}}{\partial t} = \mathcal{D}\frac{\partial^2 c_{um}}{\partial x^2} + \dot{g}\left(\frac{c_{uf}}{c_f} - \frac{c_{um}}{c_m}\right) \tag{5}$$

$$\frac{\partial c_{uf}}{\partial t} = -\dot{g}\left(\frac{c_{uf}}{c_f} - \frac{c_{um}}{c_m}\right) \tag{6}$$

These two equations along with the boundary conditions

$$\left.\frac{\partial c_{um}}{\partial x}\right|_{x=0} = \left.\frac{\partial c_{um}}{\partial x}\right|_{x=L} = 0 \tag{7}$$

and the initial conditions

$$\begin{aligned} &c_{um} = c_{uf} = 0 && \text{for} \quad |x - x_0| > \omega/2 \\ &c_{um} = \alpha c_m \quad \text{and} \quad c_{uf} = \alpha c_f && \text{for} \quad |x - x_0| < \omega/2 \end{aligned} \tag{8}$$

constitute a complete dimensional statement of the problem. x_0 and ω are the position and the width of the slit, respectively, and L is the cell length. Here, α represents the fraction of the total actin concentration in the band that is uncaged (with uniform incorporation of injected labeled actin into the endogenous cytoskeleton, and a 100% conversion of labeled actin in the band, α is simply the ratio of injected to total actin).

Nondimensional problem

Introducing the scaling

$$c_m^* = \frac{c_{um}}{\alpha c_m} \quad c_f^* = \frac{c_{uf}}{\alpha c_f} \quad t^* = \frac{t\mathcal{D}}{L^2} \quad x^* = \frac{x}{L}. \tag{9}$$

Eqs. 5 and 6 become

$$\frac{\partial c_m^*}{\partial t^*} = \frac{\partial^2 c_m^*}{\partial x^{*2}} + \gamma\beta(c_f^* - c_m^*) \tag{10}$$

$$\frac{\partial c_f^*}{\partial t^*} = -\beta(c_f^* - c_m^*) \tag{11}$$

with the parameters $\beta = L^2\dot{g}/c_f\mathcal{D}$ and $\gamma = c_f/c_m$.

The nondimensional form of the system suggests that the spatial and temporal evolution of the fluorescent populations depend upon the four parameters γ, β, ω/L, and x_0/L. The last two parameters are geometrical parameters that can be selected before an experiment. In general, however, γ and β are not known a priori. The parameter γ gives the ratio of polymerized to depolymerized actin. A physical interpretation for β can be obtained by observing that $L^2/\mathcal{D}$ is a characteristic time for free diffusion (based on the cell length) and that $c_f/\dot{g}$ is the characteristic residence time of a monomer in the filamentous pool, i.e., the filament turnover time. Therefore, β compares the time scales of the monomer diffusion and filament turnover processes.

Solution

An analytical solution of the coupled system of Eqs. 10 and 11 was found by using a Fourier-Laplace transform (see Appendix for the details of this procedure). The

results are

$$c_m^* = \frac{\omega}{L} + \sum_{k=1}^{\infty} \bar{c}_m^* \cos k\pi x^* \qquad (12)$$

$$c_f^* = \frac{\omega}{L} + \sum_{k=1}^{\infty} \bar{c}_f^* \cos k\pi x^*$$

with the Fourier coefficients given by

$$\bar{c}_m^* = \bar{c}_0^* \frac{(s_1 + \gamma\beta + \beta)e^{s_1 t^*} - (s_2 + \gamma\beta + \beta e)^{s_2 t^*}}{(s_1 - s_2)} \qquad (13)$$

$$\bar{c}_f^* = \bar{c}_0^* \frac{\mathcal{A}}{(s_1 - s_2)} \qquad (14)$$

where

$$\mathcal{A} = (s_1 + \beta + (\pi k)^2 + \gamma\beta)e^{s_1 t^*} - (s_2 + \beta + (\pi k)^2 + \gamma\beta)e^{s_2 t^*}$$

Here $\bar{c}_0^*$ represents the Fourier transform of the initial distribution of fluorescent monomer (or polymer), s_1 and s_2 are the roots of quadratics in the wave number $(\pi k)^2$ (see Eqs. A.6 and A.2 in the Appendix).

Note that it is the sum of the fluorescence contributions of the two pools that is recorded in experiments. Assuming that the fluorescence is proportional to dye concentration and the intensity of excitation light, the fluorescence intensity F can be written as

$$F = I_0 Q(c_{uf} + c_{um}) \qquad (15)$$

where I_0 and Q are the excitation light intensity and the fluorescence quantum efficiency, respectively. Using Eq. 9, the definition of γ, and normalizing with the maximum fluorescence F_0, we obtain a nondimensional fluorescence:

$$F^* = \frac{F}{F_0} = \frac{1}{1 + \gamma}(c_m^* + \gamma c_f^*). \qquad (16)$$

RESULTS

Concentration and fluorescence profile

We programmed Eqs. 12 and 16 to obtain the spatial and temporal evolution of fluorescence in the cell. A minimum of 400 terms was used in the calculations (sufficient to resolve short time solutions in the area of the slit).

A sample solution is given in Fig. 2. In this example, the fluorescent monomer population quickly diffuses away from the photoactivated band and the fluorescent filament population lags behind. Because the overall fluorescence is a weighted sum of these two, it lies between them. Note that the areas under the curves remain equal to ω/L, indicating conservation of the fluorescent species.

Center-line decay

As seen in Fig. 2, the maximum dynamic contrast in fluorescence over the course of an experiment (i.e., the difference between the initial and final fluorescence values) is obtained by making measurements at the slit center line. We therefore perform a parameter study by examining the evolution of center line fluorescence for different values of the parameters. The behavior of center line decay curves with varying β is given in Fig. 3. For our purposes here, β may be thought of as an index of filament turnover with high β indicating more rapid turnover. Note that the decay is clearly biphasic. For small times, all curves appear similar to the $\beta = 0$ curve. This curve corresponds to the case of no filament turnover. Without exchange between the two pools, the fluorescence contribution from the filaments is not dissipated. The final fluorescence level is given by Eq. 16 with $c_m^* = \omega/L$ and $c_f^* = 1$. The decay here is simply due to monomer diffusion out of the slit. Physically, the biphasic nature of the curves can be understood in the following way. Immediately after the creation of the photoactivated band, there exists a pool of unpolymerized fluorescent monomer among the filaments. This pool is free to diffuse and gives the initial rapid drop in fluorescence observed in Fig. 3. This region is termed the *diffusion regime*. For longer times, curves separate under the influence of β, which can be thought of as an index of filament turnover with high β indicating rapid turnover. The long-term fluorescence decay is due to the liberation of fluorescent actin subunits from the filamentous pool and their subsequent diffusion. This region is termed the *turnover regime*.

As β becomes large compared with one, filament turnover is rapid compared with the time required for a fluorescent monomer to diffuse a distance L. In this limit, the concentration of fluorescent subunits in the polymerized and unpolymerized pools becomes equal. The rate of decay of fluorescence is now only dependent on the size of the diffusable monomeric pool compared with the size of the immobile filamentous pool (i.e., only dependent on γ). This behavior is seen in Fig. 3 where the decay becomes independent of β for $\beta \gg 1$.

Diffusion regime

The diffusion regime indicated in Fig. 3 is shown enlarged in Fig. 4. On this scale, it is clear that the early fluorescence decay is not truly independent of β. However, the dependence is weak enough that for a short period of time the free diffusion curve (curve $\beta = 0$ discussed in the previous section) can be thought as representative of any $\beta > 0$ curve. Any experimental curve can therefore be fit to the $\beta = 0$ curve to measure the diffusive properties of actin monomer. The time window over which this approximation is valid to within a 10% uncertainty is written as $t_{10\%}^*$ and is indicated in Fig. 4.

Because the diffusion regime represents an opportunity to probe the diffusion properties of the monomer population,

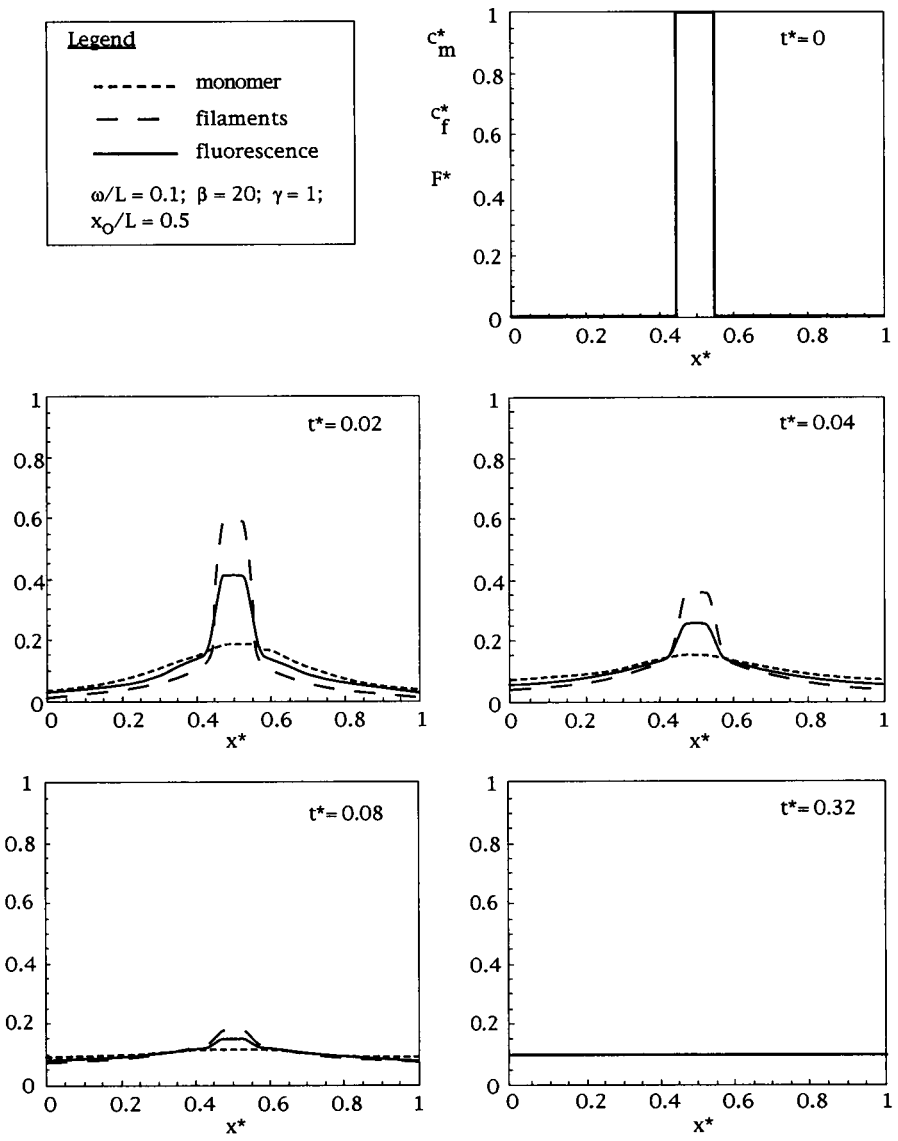

FIGURE 2 Evolution of the fluorescence and the filament and monomer concentration profiles. The parameters were chosen as $\gamma = 1$, $\beta = 20$, $\omega/L = 0.1$, and $x_0/L = 0.5$.

the model has been used to study how this regime extends if one varies the design parameters ω/L and x_0/L. As shown in Fig. 5, as long as the slit remains approximately one slit width from the end of the cell, $t^*_{10\%}$ is independent of the slit position. It is not surprising that $t^*_{10\%}$ grows when the fluorescent strip is near the end since diffusion will then only be in one direction. Note that the duration of the diffusion regime, measured by $t^*_{10\%}$, increases with ω/L. Note, however, that increasing ω/L will decrease the dynamic range of the data. This can be understood from the case $\omega/L \rightarrow 1$, for which the fluorescence no longer decays because the entire cell has been uniformly uncaged.

Turnover regime

The behavior of the fluorescence for long times can be examined by using the analytical solution restricted to small wave numbers (we used $k = 1$ in this development). With this, $s_1 - s_2$ reduces to

$$s_1 - s_2 = \pi^2 + \beta\gamma + \beta \tag{17}$$

As a consequence, $|s_2| > |s_1|$ so that for long times terms with an s_2 exponent in Eqs. 13 and 14 drop faster than terms with an s_1 exponent. With this observation, and after renormalizing the fluorescence values according to

$$F_2^* = \frac{F^* - \omega/L}{1 - \omega/L} \tag{18}$$

the long-time center-line fluorescence decay becomes

$$F_2^* = \frac{\gamma}{1+\gamma}\left(1 + \frac{(\beta + s_1)(1 + 1/\gamma)}{\pi^2 + \beta\gamma + \beta}\right)e^{s_1 t^*}. \tag{19}$$

Developing s_1 (defined in Eq. A.6) to first order with the

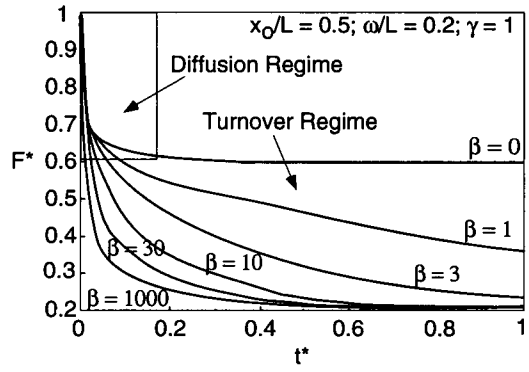

FIGURE 3 Decay of fluorescence at the slit center line. The initial fast decay of fluorescence is caused by the diffusion of uncaged actin monomers away from the slit. The long-term fluorescence decay is governed by filament turnover.

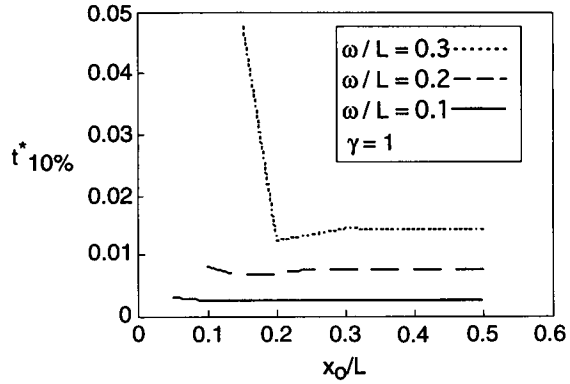

FIGURE 5 The duration of the diffusion regime with varying slit position and width. $t^*_{10\%}$ is constant for a given ω/L until about one slit width from the wall.

criterion $\beta \ll \pi^2/(1 + \gamma)$ reduces Eq. 19 to

$$F_2^* = \frac{\gamma}{1 + \gamma} e^{-\beta t^*}. \quad (20)$$

This is an extremely convenient expression because it suggests that if the turnover rate is sufficiently slow ($\beta \ll \pi^2/(1 + \gamma)$), the logarithm of the fluorescence intensity should drop linearly in time with a $-\beta$ slope, giving a direct measure of the rate of filament turnover. Furthermore, extrapolating the turnover regime decay to zero time gives $\ln(\gamma/(\gamma + 1))$, a direct measure of the ratio of polymerized to depolymerized actin. Note that in general roughly half of the actin in cells is polymerized so that $\gamma \approx 1$, and the criterion can be stated as $\beta \ll 4$ (Bray and Thomas, 1976; Condeelis, 1992). Simulations have shown that the criterion can actually be applied up to $\beta = 4$ with little error. Assuming a monomer diffusion coefficient of 10^{-7} cm^2/s (Wang et al., 1982), and a cell length of 30 μm, the criterion applies for filament turnover times longer than ~1 min. One estimate of filament turnover times in living cells can be obtained from studies of microinjected fluorescently labeled actin (Kreis et al., 1979; Taylor and Wang, 1978). These studies have found that the injected actin incorporates into all levels of the cytoskeleton in <30 min, suggesting Eq. 20 will have great value in practice.

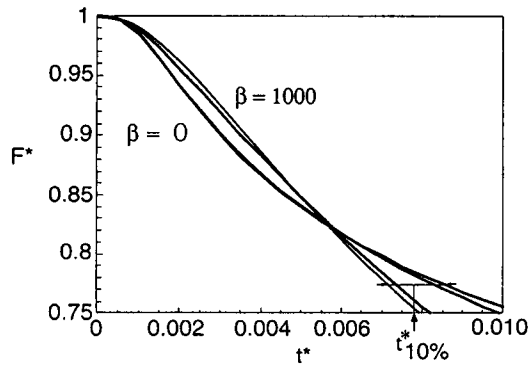

FIGURE 4 The diffusion regime. Enlargement of the diffusion regime indicated in Fig. 3 where all curves appear similar because of a weak dependence on β. β = 0, 1, 30, and 1000 are shown. ω/L = 0.1.

DISCUSSION

A continuum model describing the steady-state dynamics of the actin cytoskeleton has been developed to aid in interpreting fluorescence decay curves obtained in PAF experiments. The model demonstrates that, despite being a complex function of four parameters, the center-line fluorescence decay should be biphasic. Immediately after the creation of the photoactivated band, rapid diffusion of freely diffusing monomer contributes to a quick drop in fluorescence (the diffusion regime). The long-term fluorescence decay is due to the liberation of fluorescent actin subunits from the F-actin network during the slower process of filament turnover (the turnover regime). In Fig. 6 we present a demonstrative PAF experiment performed on a resting endothelial cell in our laboratory. The behavior is clearly biphasic as predicted by the model. Similarly, Wang et al. (1982) and Kreis et al. (1982) have noted biphasic recovery in FRAP experiments. They attributed the rapid initial recovery (order of seconds) followed by a long-term recovery (order of minutes) to the presence of populations of differing diffusivities. Filaments would seem the likely identity of the second population. However, morphological descriptions of the actin cytoskeleton indicate nearly all cortical filaments are interconnected via filament cross-linking proteins (Hartwig and Shelvin, 1986), and therefore are likely immobile on the time scales of these experiments. In this paper, we present a mathematical model of PAF experiments that suggests this behavior is due to a transient burst of free monomer diffusion superimposed upon a slower decay due to filament turnover.

Our model can be used to extract quantitative information about actin dynamics from PAF or FRAP data records. In

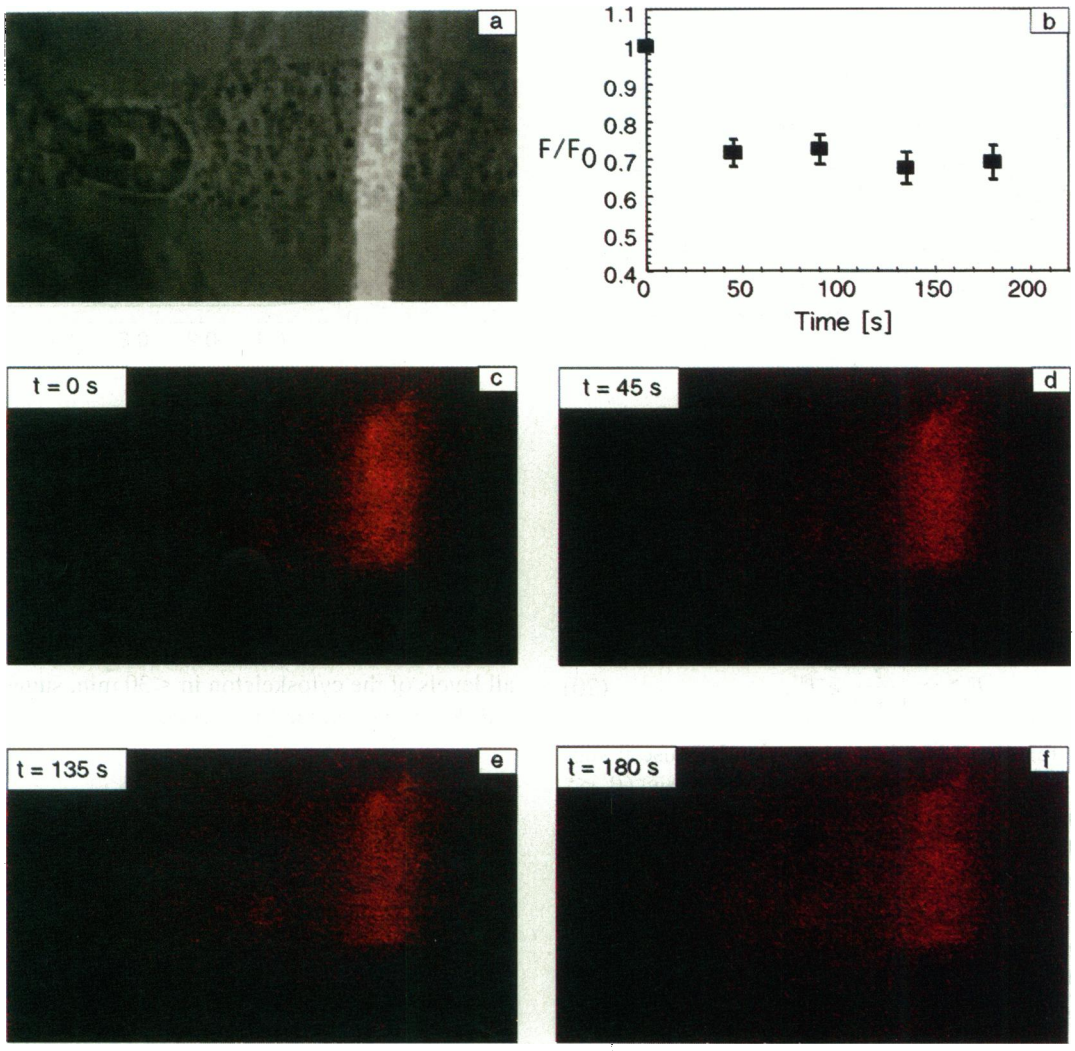

FIGURE 6 PAF experiment for a resting endothelial cell. This sequence was obtained by microinjecting cells with caged resorufin-iodoacetamide-labeled actin (synthesized according to Theriot and Mitchison (1991)) and recording the fluorescence with a PAF system modeled after that of Mitchison (1989). (*a*) Phase-contrast image of the cell superimposed with the uncaging UV band. (*b*) Center line fluorescence decay curve obtained from the following sequence of fluorescent images, (*c* to *f*). The decay is clearly biphasic, suggesting rapid monomer diffusion followed by a slow decay due to filament turnover. The photoliability of the fluorophore demanded a low sampling frequency and a short data record to minimize bleaching; therefore, we do not attempt to infer parameters from this data. Errors on measured values were computed by considering system signal-to-noise ratio and pixel counts.

particular, a time window can be obtained immediately after photoactivation where the fluorescence decay retains the character of free monomer diffusion. In vivo actin monomer diffusion coefficient estimates have been obtained in the FRAP studies of Wang et al. (1982), and Kreis et al. (1982). The procedure used to determine diffusion coefficients from data records relates the time for 50% fluorescence recovery to the diffusion coefficient (Axelrod et al., 1976). The present theory is in agreement with this interpretation so long as measurements are made wholly in the diffusion regime. This interpretation of the measurements will contain significant error, however, if the transition between the diffusion and turnover regimes occurs before 50% fluorescence levels have been reached. This reasoning may explain the significant variability in actin monomer diffusion coefficient estimates obtained in these studies ($10^{-9} - 10^{-7}$ cm^2/s).

A careful analysis of the long-term fluorescence decay suggests this region can be studied to measure the ratio of polymerized to unpolymerized actin and the filament turnover rate (γ and β). A particularly simple analysis was shown to result for $\beta < 4$, which is thought to be a reasonable physiological limit.

The utility of our model is restricted by the idealizations used in formulating it (assumptions 1–5). The assumptions of uniform monomer exchange rates and actin concentrations throughout the cell are likely places where the model may be improved. The geometrical constraints can be relaxed if the governing equations are solved analytically. The steady-state assumption currently restricts application to situations where significant polymerization or depolymerization is not occurring. The work presented here, however, represents the first attempt at a mathematical framework for

the quantitative interpretation of PAF and FRAP experiments on cytoskeletal proteins.

In summary, the model developed here provides a new interpretation of the fluorescence time course in PAF and FRAP studies. The model provides a means for the simultaneous measurement of three important parameters governing the dynamics of the actin cytoskeleton: monomer diffusion coefficients, filament turnover rates, and the ratio of polymerized to unpolymerized actin.

APPENDIX

Detailed solution

To solve our coupled system of second order differential equations (Eq. 10 and 11), we used the Fourier-Laplace transform defined as

$$\bar{\bar{f}}(k, s) = \int_0^\infty dt \int_0^1 dx f(x, t)\, e^{-st} e^{-i\pi kx} \qquad (A.1)$$

(The superscript = denotes the double Fourier and Laplace transform.)

The following algebraic system is obtained:

$$\begin{bmatrix} (s + (\pi k)^2 + \gamma\beta) & -\gamma\beta \\ -\beta & (s + \beta) \end{bmatrix} \begin{bmatrix} \bar{\bar{c}}_m^* \\ \bar{\bar{c}}_f^* \end{bmatrix} = \begin{bmatrix} \bar{c}_0^* \\ \bar{c}_0^* \end{bmatrix} \qquad (A.2)$$

where $\bar{c}_0^*$ is the Fourier transform of the initial conditions. With the initial conditions given by Eq. 8, it can be verified that

$$\bar{c}_0^* = \frac{2}{\pi k}\left[\sin\left(k\pi\left(\frac{x_0}{L} + \frac{\omega}{2L}\right)\right) - \sin\left(k\pi\left(\frac{x_0}{L} - \frac{\omega}{2L}\right)\right)\right] \qquad (A.3)$$

This system can then be solved for $\bar{\bar{c}}_f^*$ and $\bar{\bar{c}}_m^*$. We obtained

$$\bar{\bar{c}}_m^* = \frac{\bar{c}_0^*(s + \beta + \gamma\beta)}{(s - s_1)(s - s_2)} \qquad (A.4)$$

$$\bar{\bar{c}}_f^* = \frac{\bar{c}_0^*\,(s + (\pi k)^2 + \gamma\beta + \beta)}{(s - s_1)(s - s_2)} \qquad (A.5)$$

$$s_1 = \frac{-(\pi k)^2 - \beta\gamma - \beta + \sqrt{((\pi k)^2 + \beta\gamma + \beta)^2 - 4(\pi k)^2\beta}}{2}$$

with

$$s_2 = \frac{-(\pi k)^2 - \beta\gamma - \beta - \sqrt{((\pi k)^2 + \beta\gamma + \beta)^2 - 4(\pi k)^2\beta}}{2}. \qquad (A.6)$$

Since they are polynomials, Eqs. A.4 and A.5 can be easily inverse Laplace transformed:

$$\bar{c}_m^* = \bar{c}_0^* \frac{(s_1 + \gamma\beta + \beta)e^{s_1 t^*} - (s_2 + \gamma\beta + \beta)e^{s_2 t^*}}{(s_1 - s_2)} \qquad (A.7)$$

$$\bar{c}^*{}_f = \bar{c}_0^* \frac{\mathcal{A}}{(s_1 - s_2)} \qquad (A.8)$$

where

$$\mathcal{A} = (s_1 + \beta + (\pi k)^2 + \gamma\beta)e^{s_1 t^*} - (s_2 + \beta + (\pi k)^2 + \gamma\beta)e^{s_2 t^*}.$$

Finally, the solution is obtained by taking the inverse Fourier transform of these two expressions. Because of the boundary condition the inverse transform reduces to a cosine transform and the final solution is

$$c_m^* = \frac{\omega}{L} + \sum_{k=1}^{\infty} \bar{c}_m^* \cos k\pi x^*$$

$$c_f^* = \frac{\omega}{L} + \sum_{k=1}^{\infty} \bar{c}_f^* \cos k\pi x^*. \qquad (A.9)$$

This work was partially supported by the Roche Research Foundation and the Whitaker Foundation.

REFERENCES

Axelrod, D., J. Koppel, E. Schlessinger, E. Elson, and W. W. Webb. 1976. Mobility measurement by analysis of fluorescence photobleaching recovery kinetics. *Biophys. J.* 16:1055–1069.

Bray, D., and C. Thomas. 1976. Unpolymerized actin in fibroblast and brain. *J. Mol. Biol.* 105:527–544.

Carlier, M. F., C. Jean, K. Rieger, M. Lenfant, and D. Pantaloni. 1993. Modulation of the interaction between G-actin and thymosin β4 by the ATP/ADP ratio: possible implication in the regulation of actin dynamics. *Proc. Natl. Acad. Sci. USA.* 90:5034–5038.

Condeelis, J. 1992. Are all pseudopods created equal? *Cell Motil. Cytoskeleton.* 22:1–6.

Giuliano, K. A., and D. L. Taylor. 1994. Fluorescent actin analogs with a high affinity for profilin in vitro exhibit an enhanced gradient of assembly in living cells. *J. Cell Biol.* 124:971–983.

Hartwig, J. 1992. Mechanisms of actin rearrangements mediating platelet activation. *J. Cell Biol.* 118:1421–1442.

Hartwig, J. H. and P. Shelvin. 1986. The architecture of actin filaments and the ultrastructural location of actin-binding protein in the periphery of lung macrophages. *J. Cell Biol.* 103:1007–1020.

Kreis, T. E., B. Geiger, and B. Schlessinger. 1982. Motility of microinjected rhodamine actin within living chicken gizzard cells determined by fluorescence photobleaching recovery. *Cell.* 29:835–845.

Kreis, T. E., K. H. Winterhalter, and W. Birchmeier. 1979. *In vivo* distribution and turnover of fluorescently labeled actin microinjected into human fibroblasts. *Proc. Natl. Acad. Sci. USA.* 76:3814–3818.

Lassing, I. and U. Lindberg. 1985. Specific interaction between phosphatidylinositol 4,5-biphosphate and profilactin. *Nature.* 318:472–474.

Mitchison, T. J. 1989. Polewards microtubule flux in the mitotic spindle: evidence from photoactivation of fluorescence. *J. Cell Biol.* 109: 637–652.

Nachmias, V. 1993. Small actin-binding proteins: the β thymosin family. *Curr. Opin. Cell Biol.* 5:56–62.

Safer, D., R. Golla, and V. Nachmais. 1990. Isolation of a 5-kD actin sequestering peptide from human blood platelets. *Proc. Natl. Acad. Sci. USA.* 87:2536–2539.

Sawin, K. E., J. A. Theriot, and T. J. Mitchison. 1992. Photoactivation of fluorescence as a probe for cytoskeletal dynamics in mitosis and cell motility. *In* Fluorescent and Luminescent Probes for Biological Activity. W. T. Mason, editor. Academic Press, New York. 405–419.

Sun, H., K. Kwiatkowski, and H. L. Yin. 1995. Actin monomer binding proteins. *Curr. Opin. Cell Biol.* 7:102–110.

Taylor, D. L., and Y. L. Wang. 1978. Molecular cytochemistry: incorporation of fluorescently labeled actin into living cells. *Proc. Natl. Acad. Sci. USA.* 75:857–861.

Theriot, J. A. and T. J. Mitchison. 1991. Actin microfilament dynamics in locomoting cells. *Nature.* 352:126–131.

Theriot, J. A. and T. J. Mitchison. 1992. Comparison of actin and cell surface dynamics in motile fibroblasts. *J. Cell Biol.* 119:367–377.

Wang, Y. L. 1985. Exchange of actin subunits at the leading edge of living fibroblasts: possible role of treadmilling. *J. Cell Biol.* 101: 597–602.

Wang, Y. L., F. Lanni, P. L. McNeil, B. R. Ware, and D. L. Taylor. 1982. Mobility of cytoplasmic and membrane-associated actin in living cells. *Proc. Natl. Acad. Sci. USA.* 79:4660–4664.

Wegner, A. 1976. Head to tail polymerization of actin. *J. Mol. Biol.* 108:139–150.